ANADOLU ÜNİVERSİTESİ BİLİM VE TEKNOLOJİ DERGİSİ –A
Uygulamalı Bilimler ve Mühendislik

ANADOLU UNIVERSITY JOURNAL OF SCIENCE AND TECHNOLOGY –A
Applied Sciences and Engineering
Cilt/Vol.:12-Sayı/No: 1 : 25-36 (2011)

FORMATION MECHANISM OF NANOSIZED TIN OXIDE (SnO_2) POWDER DURING HYDROTHERMAL SYNTHESIS

M. Ozan ÖZER [1], Ender SUVACI*, Aydın DOĞAN

ABSTRACT

Preparation of nanosized SnO_2 electroceramic powders via hydrothermal synthesis was investigated as a function of initial concentration and treatment time in order to understand the formation and growth mechanisms. SnO_2 powder was successfully synthesized from the hydrous tin oxide by hydrothermal synthesis at 200°C. Crystalline SnO_2 particles with a specific surface area as high as 170 m^2/g were produced in a single step without requiring any calcination process. As initial concentration of metal cation increases from 0.0125 to 0.05 M, an Ostwald ripening type growth process was observed in the crystallite size from 3.1 to 4.6 nm. Evolution of tin oxide particles was also investigated by altering the treatment time from 1 to 24 h and a diffusion controlled growth behavior was observed as a function of synthesis time.

Keywords: Tin oxide, Hydrothermal synthesis, Nanosized particle.

HIDROTERMAL SENTEZ SÜRECINDE NANO BOYUTLU KALAY OKSITIN(SnO_2) OLUŞUM MEKANIZMASI

ÖZ

Nano boyutlu SnO_2elektroseramik tozların hidrotermal yöntemle üretimi, tozların oluşum mekanizmasını anlamak üzere başlangıç derişimi ve işlem süresinin bir fonksiyonu olarak incelendi. SnO_2 tozları hidrotermal yöntemle su içeren kalay oksitten 200^0C de başarıyla sentezlendi. 170 m^2/g a kadar spesifik yüzey alanınasahip kristal SnO_2 tozları kalsinasyon gerektirmeden tek basamakta üretildi. Başlangıç metal katyon derişimi 0.0125 den 0.05 M a çıkarıldığında Ostwald irileşmesi türünde bir büyüme süreciyle kristalit boyutunun 3.1 den 4.6 nm ye çıktığı gözlendi. Kalay oksit partiküllerinin oluşumu 1 ile 24 saat aralığında değiştirilerek incelendi ve sentez süresinin bir fonksiyonu olarak difüzyon kontrollü büyüme davranışı tespit edildi.

Anahtar Kelimeler: Kalay oksit, Hidrotermal sentezi, Nano boyutlu parçacık.

---

[1], Anadolu University, Department of Materials Science and Engineering, Iki Eylul Campus, 26480 Eskisehir, Turkey.
*Corresponding Author: Tel:+90-222-3213550/ext.6386; Fax:+90-222-3239501 E-mail: esuvaci@anadolu.edu.tr or esuvaci@yahoo.com

Recieved: 2 November 2010; **Revised:** 2 December 2010; **Accepted:** 30 March 2011

1. INTRODUCTION

Tin oxide (SnO_2) is an important semiconducting material which has been widely used in an extensive range of applications including catalysts (Seiyama et al., 1972; Caldadararu et al., 1995), gas sensors (Seiyama et al., 1962; Taguchi, 1962), varistors (Henrich and Cox, 1994; Pianaro et al., 1995), transparent electrodes (Chopra et.al, 1983; Dawar, and Joshi, 1984), and optoelectronic devices (Aoki and Sasakura, 1970). SnO_2-based gas sensors are the most widely utilized ones, among the semiconducting oxides. They play critical role in detection of flammable or reducing gases such as carbon monoxide, hydrogen and methane at low level concentrations in many industrial applications (Ihokura and Watson, 1994; Yamazoe et al., 1979; Ihokura, 1981; Xu et al., 1990; . Moulson and Herbert, 1990). Since the gas sensing property of such materials depends on effective surface area, controlling the crystallite size and hence surface area, which can be done by selecting a proper synthesis method, is very critical for a high performance gas sensor fabrication.

Tin oxide, used for gas sensors, has been synthesized by various synthesis methods such as direct strike and homogeneous precipitation (Song and Kang, 2000; Nitta and Otani, 1980), two-step solid state synthesis (Li and Chen, 2002), microemulsion (Song, and Kim, 1999), sol-gel (Zhang and Liu, 1999), spray pyrolysis (Lee and Park, 1993), gel combustion (Bhagwat et al., 2003) and hydrothermal synthesis (Hirano, 1987; He and Li, 1999). Among these methods, conventionally accepted ones are chemical solution synthesis methods including direct strike and homogeneous precipitation methods. The main drawback of these two methods is requirement of a calcination step, which results in aggregation and thermal growth of fine synthesized particles. Hydrothermal synthesis involves the treatment of aqueous solutions or suspensions of precursor particles usually at elevated temperatures and pressures. The reactions occurring in hydrothermally treated solutions of inorganic compound can produce fine, high purity and homogeneous metal oxide particles usually in a single step process without requiring any further thermal treatment (Hirano, 1987).

In the literature, most of the previous hydrothermal studies are based on the standard synthesis of tin oxide and changing some processing variables such as temperature, concentration and treatment time to change particle characteristics (He and Li, 1999; Baik and Sakai, 2000; Baik et al., 2000; Zhang, 2003; Vuong et al., 2004). Although those processing parameters have been investigated to date, it is still not clear that how the particles form and grow in this system. Therefore, the objective of this study was to determine the formation mechanism of tin oxide particles during the hydrothermal process via systematically evaluating the effects of concentration and treatment time on the physical characteristics of the SnO_2 powder in the hydrothermal synthesis.

2. EXPERIMENTAL PROCEDURE

In the current study, hydrated tin oxide gel was used as a precursor for the hydrothermal process. It was prepared by homogeneous precipitation of HMT added $SnCl_4$ solution. Concentrations of both HMT and $SnCl_4$ were in the range of 0.025 - 0.1 M. After washing with distilled water for five times, the precipitated hydrous tin oxide gel was suspended in an aqueous ammonium hydroxide (NH_4OH) solution at pH 12, by adjusting hydrous tin oxide concentration ranging between 0.0125 - 0.05M and subjected to a hydrothermal treatment at 200^oC for 24 h in a 600 ml autoclave (Parr Ins. Co., Pressure Reactor PARR4842). Particle evolution was monitored by interrupting the experiments after 1, 5, 10 and 15 h reaction times. Hydrothermal synthesis was followed by drying stage at 90^oC for 24-72 h in a drying oven. Figure 1 shows the process flow chart, which was utilized to synthesize tin oxide particles by hydrothermal synthesis method in this study.

Phase development was monitored by Fourier-transformed infrared spectroscopy (FTIR, Bruker, Tensor 27) and x-ray diffraction (XRD, Rigaku-Rint 2200) techniques. Samples were dried at 90^oC for 72 h and diluted with KBr and pressed into a disk shape prior to FTIR analyses. Thermochemical behavior of the synthesized powder was characterized by thermogravimetric (TGA) and differential thermal (DTA) analyzers (Netzsch, STA 409 PG).

XRD measurements were carried out between $20\text{-}70^o$ with 2^o/min. The crystallite size of the produced tin oxide samples was calculated by means of x-ray line broadening measurement according to Scherrer equation (Cullity, 1978):

$$D = \frac{0.9\lambda}{\beta\cos\theta} \qquad (1)$$

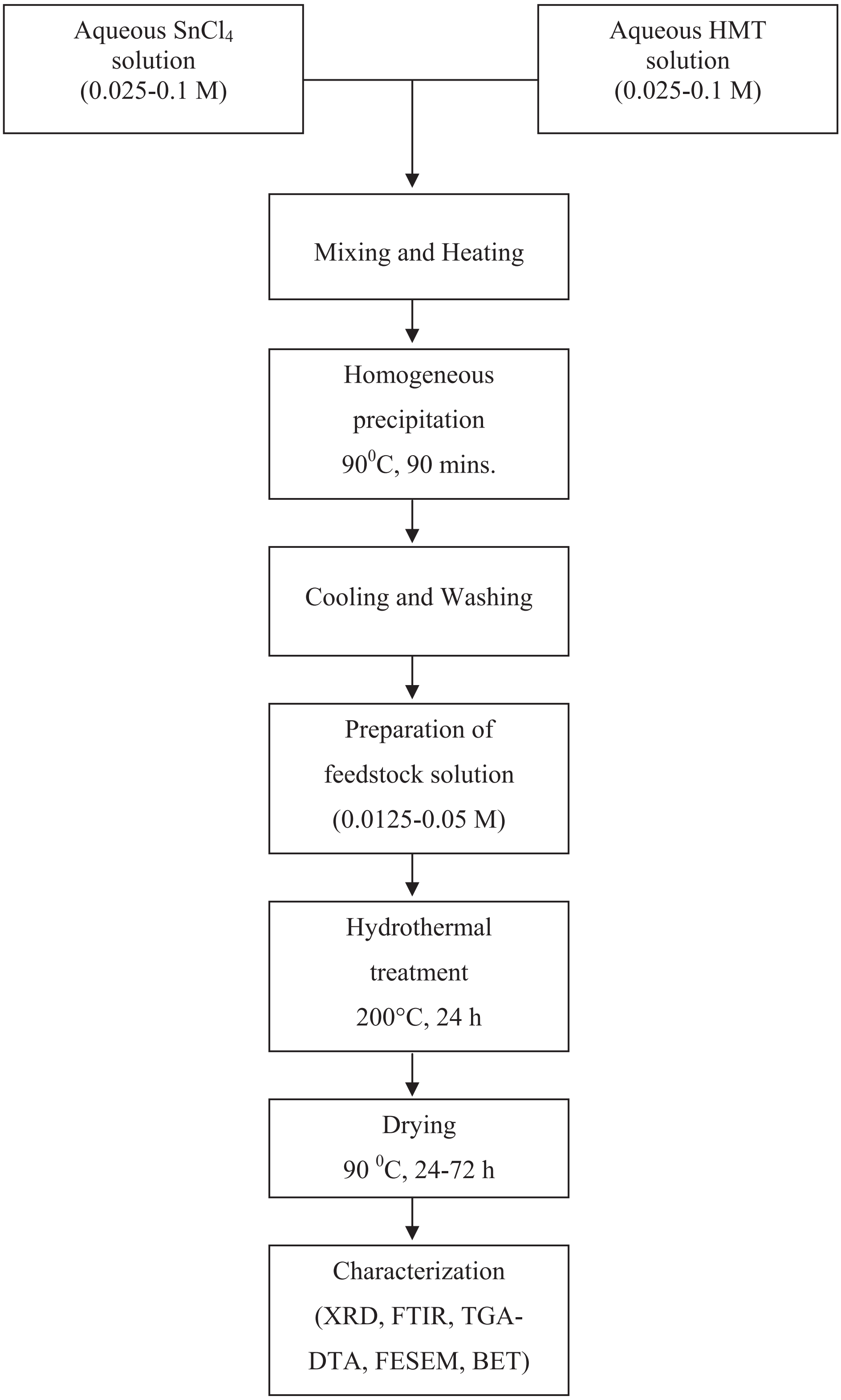

Figure 1. The process flow chart used for synthesis of nanosized SnO_2 powders by hydrothermal synthesis.

where D, mean crystallite size, λ, wavelength (i.e., 1.5418 Å for Cu Kα), β, full width half maximum of SnO_2 (110) line after instrumental broadening effects are eliminated and 2θ, diffraction angle for the (110) line (in radian). Specific surface area of the powder was measured by a gas adsorption (Brunauer-Emmett-Teller, BET, Quantachrome Ins., Autosorb-1C) technique after degassing at 150ºC for 2 h. Morphological characteristics of the prepared powders were observed by field emission scanning electron microscope (FESEM, Zeiss 50 Supra VP).

3. RESULTS AND DISCUSSION

3.1 Phase Development

XRD pattern of 0.025 M SnO_2 powder after 24 h hydrothermal treatment is shown in Figure 2. This pattern confirms formation of crystalline SnO_2 powders from hydrous tin oxide after hydrothermal synthesis at 200ºC for 24 h. High level of noise in the XRD pattern can be attributed to very fine crystallite sizes and/or residual hydroxide content. FTIR analysis was utilized to investigate the existing bonds in the synthesized powder (Fig. 3). The peak occurs at about 660 cm^{-1} in the FTIR pattern indicates formation of O–Sn–O bonds during the hydrothermal synthesis. The peak occurs at about 1620 cm^{-1} belongs to H–OH bonds probably coming from moisture content of the powder, peaks at 3400, 1250, 1180, 960 and two peaks at 2400 cm^{-1} can be attributed to Sn–OH bonds (Popescu and Verduraz, 2001). Peaks at 1380 and 3150 cm^{-1} belong to –NH stretching and –NH deformation ammonia, respectively (Socrates, 1980). These results indicate that synthesized powder is tin oxide containing some degree of moisture, residual hydroxide and some ammonia content. Residual hydroxide content is an indication of either incomplete conversion of hydrated tin oxide or some reaction between SnO_2 and H_2O due to very high surface area of the synthesized powder and the residual ammonia is coming from ammonium hydroxide (NH_4OH) solution probably due to inadequate washing step after the hydrothermal synthesis.

Figure 4 demonstrates TGA and DTA data for the 0.025 M SnO_2 powder. Total weight loss occurs in four stages as shown in the TGA data: First, 5% weight loss is observed at $T < 150$ºC due to physically adsorbed water which appears as an endothermic peak in the DTA data (Fig. 4). From the FTIR result, it can be estimated that the strong exothermic peak, which corresponds to 1% weight loss, around 200°C in the DTA curve is due to decomposition of the residual ammonia. A similar result was also observed by K. C. Song and Y. Kang (Song and Kang, 2000). Second exothermic peak, which corresponds to 1.5% weight loss, around 375°C was predicted as decomposition of an organic impurity which is probably coming from PTFE (polytetrafluoroethylene) lining of the autoclave. Chemically adsorbed water (hydroxide group) is eliminated from the system between 380-800ºC, resulting approximately 2.5% weight loss. This thermogravimetric behavior of the powders is consistent with the literature, in which N.S. Baik et al. found that the hydrothermal treatment eliminates weakly bonded water molecules, reducing the total amount of dehydration. Similar to this study, although the amount of dehydration was much less in the hydrothermally treated solutions (Baik et al., 2000) with respect to other direct precipitation systems (Song and Kang, 2000), it could not be eliminated totally.

24 h treated 0.025 M SnO_2 powder has a surface area of 166 m^2/g from the BET analysis and hence equivalent spherical diameter is calculated as 5.3 nm. On the other hand, crystallite size is calculated by x-ray line broadening as 3.4 nm. Small difference in the particle size results between x-ray line broadening and BET analysis can be attributed to agglomerate formation in the system. As-prepared nanosized tin oxide powder has a tendency of agglomeration in order to reduce such a high surface area (166 m^2/g). Agglomeration of the as-prepared tin oxide powder is also confirmed by the SEM. Figure 5 shows the SEM micrograph for the 0.025 M SnO_2, which has a homogeneous microstructure consisting of spherical agglomerates of fine tin oxide particles with a narrow particle size distribution. In a similar hydrothermal study, N.S. Baik et al. (Baik et al., 2000) synthesized particles at 6 nm from 0.9 wt % sol solution which corresponds to approximately 0.033 M. This is an evidence of the suitability of hydrothermal synthesis to produce controlled particles in terms of particle size and morphology.

3.2 Effect of Initial Concentration on Powder Characteristics

Effect of the initial hydrous tin oxide concentration on the crystallite size and the specific surface area of the synthesized powder is demonstrated in Figure 6. Average crystallite size was calculated as 4.6, 3.4 and 3.1 nm for the 0.05, 0.025 and 0.0125 M SnO_2, respectively.

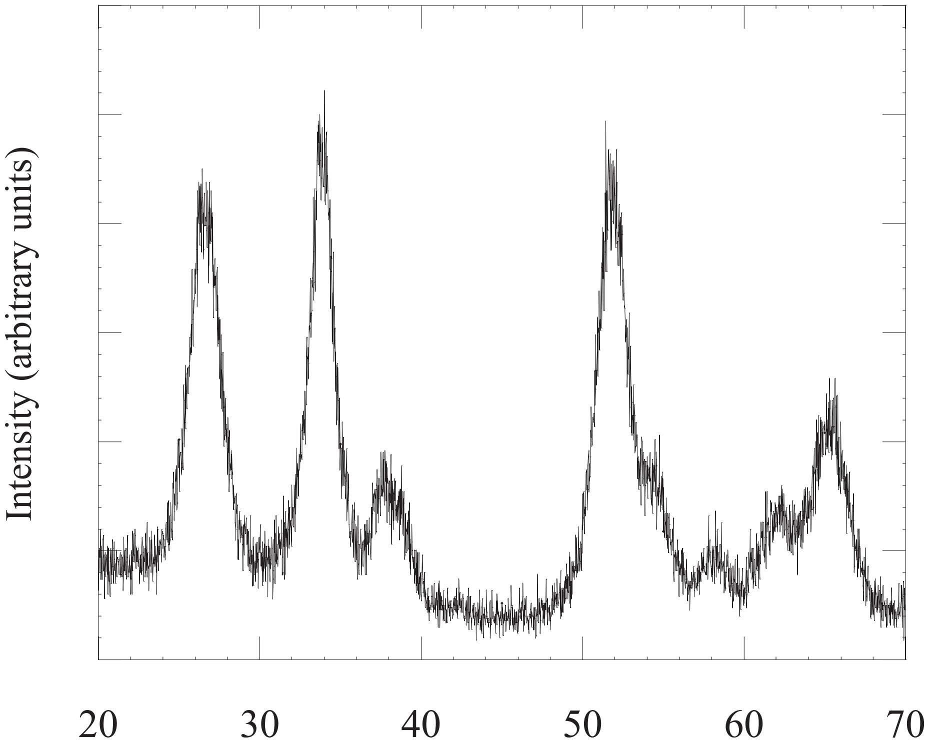

Figure 2. XRD pattern of 24 h hydrothermally synthesized 0.025M SnO_2 powder

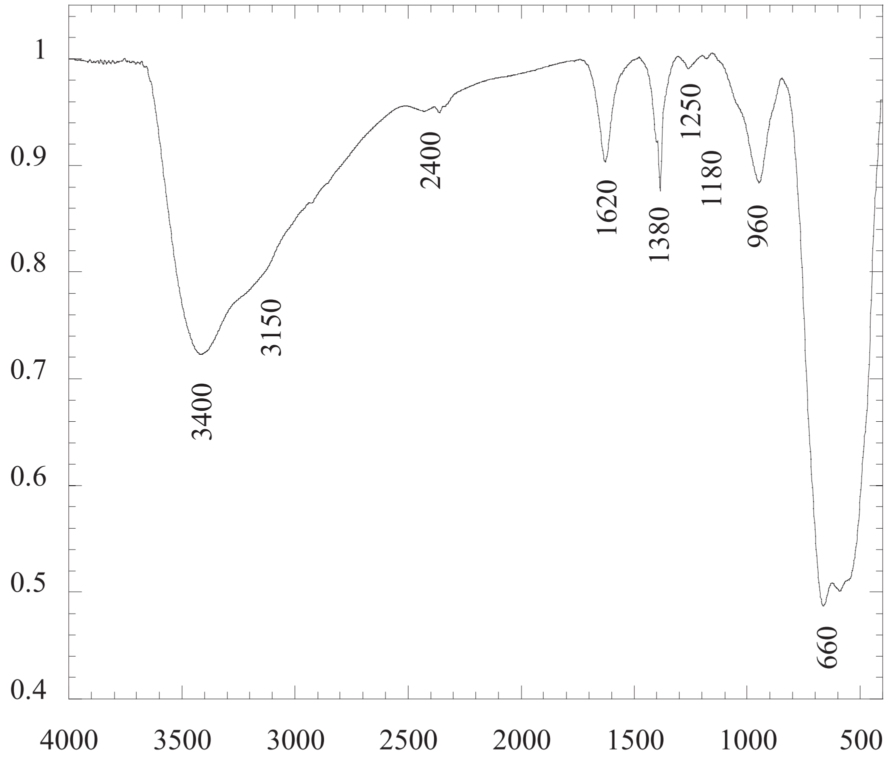

Figure 3. The FTIR plot of 24 h synthesized 0.025 M SnO_2 powder after 72 h drying at 90°C

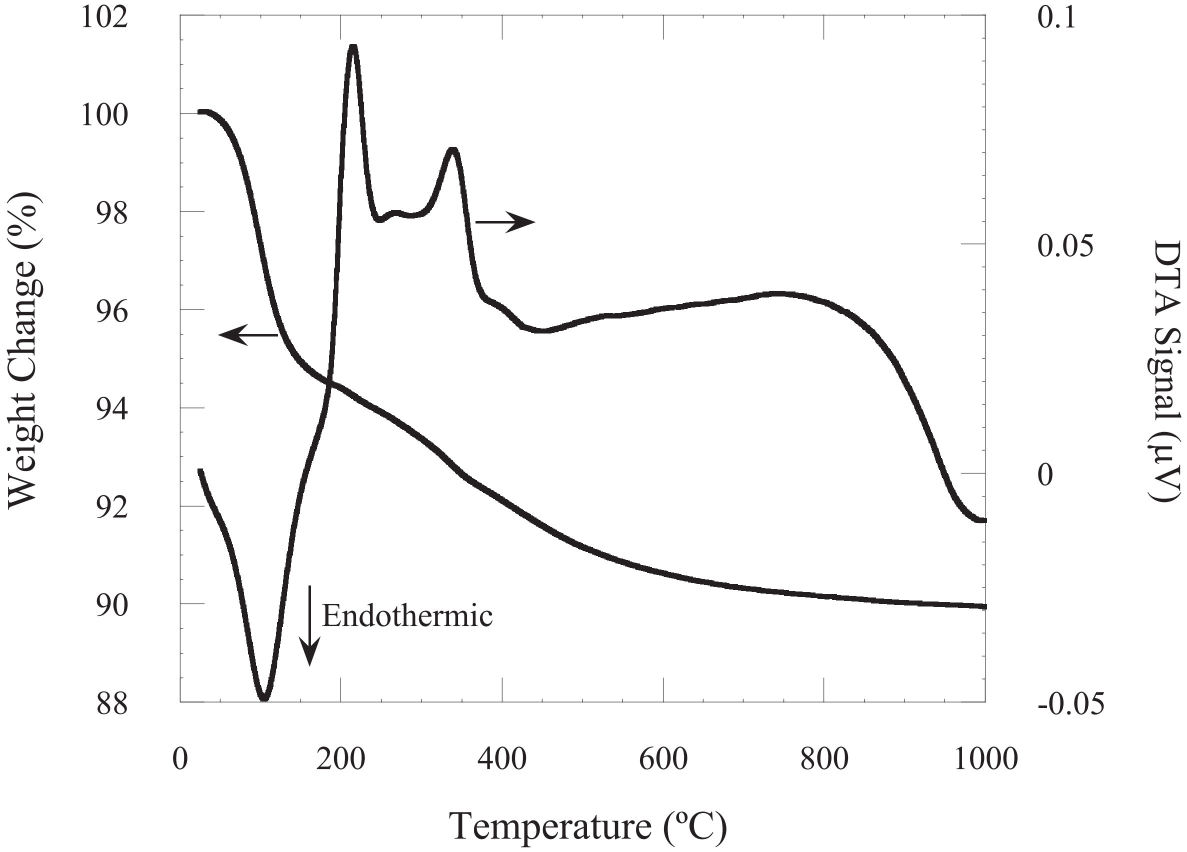

Figure 4. TG and DTA curves of 24 h synthesized 0.025M SnO_2 powder

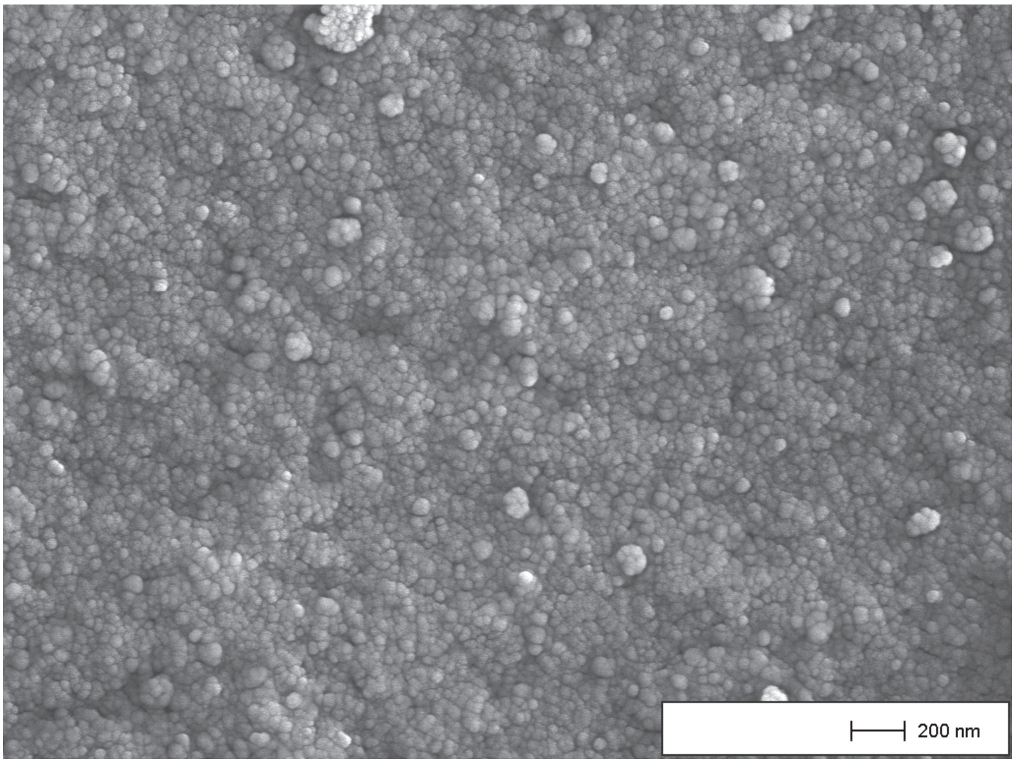

Figure 5. SEM micrograph of the SnO_2 powder synthesized at 200°C, 24 h

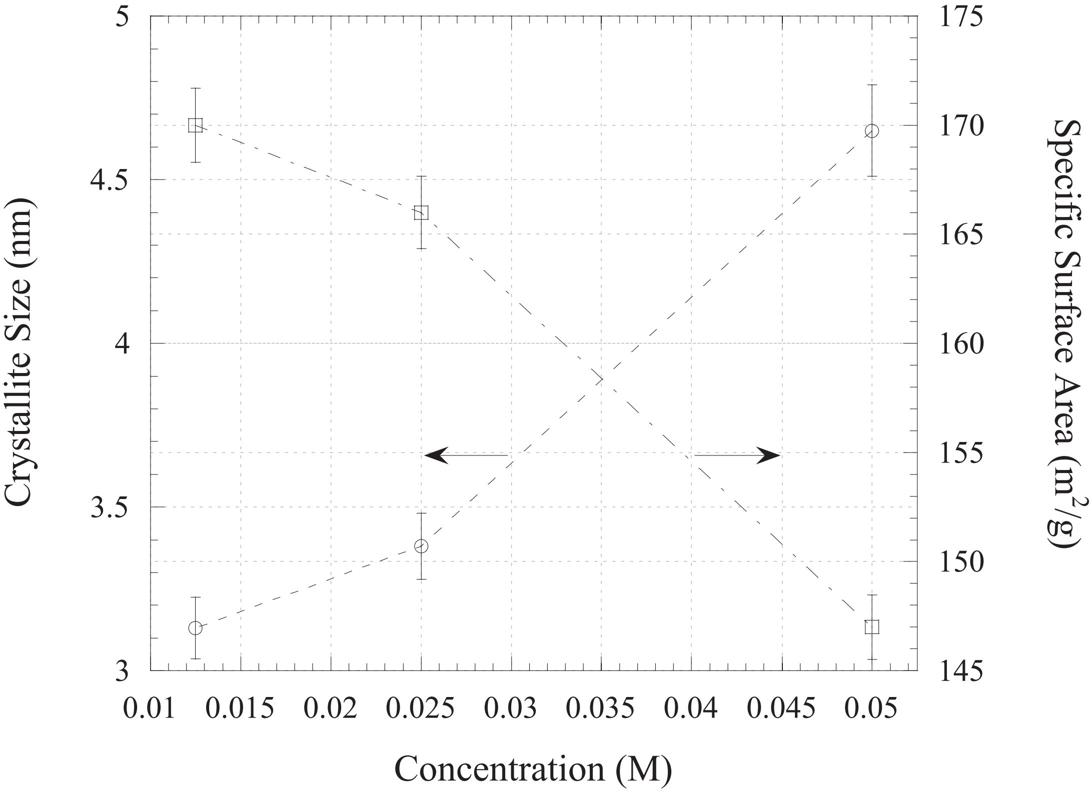

Figure 6. Effect of the initial concentration on the crystallite size and specific surface area of the SnO_2 powder.

This behavior does not obey the classical nucleation and growth theory in which the higher concentration should result finer particle sizes due to increase in the quantity of nuclei in the case of homogeneous nucleation (Nielsen, 1964). One possible scenario to explain the observed behavior is that, theoretical approach could not be observed because of changing supersaturation ratio throughout the synthesis. This behavior can be explained by Thomas Kelvin equation which describes the saturation ratio *(S)* at which particles of size r^* will dissolve.

$$S\left(r^*\right)=\exp\left(\frac{2\beta_a}{3r^*\beta_\upsilon}\frac{\gamma\hat{V}}{R_gT}\right) \tag{2}$$

where, β_υ and β_a are the volume and surface area conversion factors, respectively, $\hat{V}$ is molar volume, γ is surface free energy, R_g is gas constant and T is temperature (Ring, 1996). When $S\text{-}S(r^*)$ is positive, particles will precipitate from solution; when $S\text{-}S(r^*)$ is negative, particles smaller than size r^* will dissolve and particles larger than r^* will grow. This dissolution of fines and precipitation on larger particles, referred to as Ostwald ripening, occurs in many batch precipitation systems because the supersaturation ratio, *S*, decreases with time as the batch precipitation proceeds. Initially, at high supersaturation, nucleation produces large numbers of fine particles. This decreases the supersaturation, preventing further nucleation and leading to slow growth, which further decreases the supersaturation ratio. When the saturation ratio falls below the critical value, $S(r^*)$, for the fine particles previously precipitated, they will dissolve holding the supersaturation ratio constant. At this constant supersaturation ratio, only particles larger than r^* will grow at the expense of all smaller particles present in the suspension (Ring, 1996).

In the current study, expected nucleation frequency would be high for high concentration (e.g., 0.05 M). As a result of that, corresponding size of primary nucleus should be small and stability of these small nuclei is low regarding to the Thomas Kelvin Equation (2). Therefore, some of these small nuclei tend to dissolve in the solution to increase the supersaturation level. After the dissolution, they prefer to precipitate on the preformed surfaces (i.e., growth on existing particles) because precipitation on a free surface is more favorable than creating a new surface in terms of activation energies. On the contrary of this, for lower concentrations (e.g., 0.0125 M) initial nucleation frequency is lower than the high concentrations and, therefore, stability of primary nuclei is higher compared to the high concentrations. Instead of dissolution in the solution, these stable nuclei tend to grow preventing further nucleation and leading to slow growth, which produces fine particles. Briefly, stability of primary nucleus can be attributed to size of primary nuclei; the coarser nuclei are evaluated as more stable because dissolution of these coarse nuclei is more difficult than dissolution of fine nuclei. Consequently, for the low concentration (0.0125 M), very fine crystallite size (3.1 nm) was obtained as a result of stable primary nucleation mechanism; however, for high concentration (0.05 M) coarser crystallite size (4.6 nm) was obtained as a result of the dissolution of some primary nuclei which are smaller than the critical size. Although similar results were also reported by Nam Seok. Baik et al. (Baik et al., 2000) that the particle size was 6 and 17 nm for 1.8 and 6.1 wt% sol suspension, respectively, the concentration effect may be limited in this study with respect to results of their study due to the range covered.

In Figure 6, surface area of the synthesized SnO_2 powder was found to be inversely related to the initial hydrous tin oxide concentration. The 0.0125, 0.025 and 0.05 M SnO_2 powders exhibit specific surface areas of 170, 166 and 147 m^2/g, respectively. Inverse relation between the initial concentration and the specific surface area of the synthesized powder was attributed to increase in crystallite size with increasing concentration.

3.3 Effect of Treatment Time and the Powder Formation Mechanism

In order to investigate the influence of treatment time on the powder characteristics, various treatment times were examined including 1, 5, 10 and 15 hours under constant hydrous tin oxide concentration (0.05 M) in NH_4OH solution. Formation of the crystalline SnO_2 powder even after 1 h synthesis was observed. Effect of treatment time on crystalline phase evolution can be monitored in Figure 7. Although produced phase remained stable (cassiterite) as a function of time, development of crystalline phase, considering the area beneath the each peak, and the crystallite size (Fig. 8) increased with increasing treatment times. For the 0.05 M SnO_2, the average crystallite size was calculated as 3.2, 3.7, 4.1, 4.2 and 4.6 nm after 1, 5, 10, 15 and 24 h treatment times, respectively. Coarsening with treatment time is explained by the growth of larger crystals at the expense of smaller crystals and is governed by capillary forces. Since the chemical potential of a particle increases with decreasing particle size, the equilibrium solute concentration for a small particle is much higher than that for a large particle. The resulting concentration gradients lead to the transport of tin cations from the small particles to larger particles. The rate law for this Ostwald ripening type process derived by Lifshitz, Slyozov and Wagner (LSW) is given by the following equation.

$$r^n - r_o^n = kt \tag{3}$$

where r is the average particle radius, r_o is the average initial particle radius, k is the rate constant, t is time and n is the power defined by growth habit. If the growth process is diffusion controlled $n = 3$ whereas, if the growth process controlled by interface reaction $n = 2$ (Lifshitz and Slyozov, 1961). Comparison of the experimental data with the Equation 3 (solid lines in Fig. 8) indicates that the experimental results fit well with the theoretical values in the case of $n = 3$, which suggests that the particle growth process is controlled by the diffusion process in this system.

Besides crystallite size, the specific surface area of the synthesized powder was affected by treatment times. For the 0.05 M SnO_2, the specific surface area was measured as 190, 165, 158, 152 and 147 m^2/g after 1, 5, 10, 15 and 24 h treatment times, respectively. This result confirms the former growth approach as a function of treatment time. In addition to the BET analysis, effect of the treatment time on particle characteristics of synthesized powder was visualized by scanning electron microscope. Figure 9 demonstrates the difference in particle characteristics between 1 and 24 h synthesized powders. This time dependent behavior is also confirmed for SnO_2 system by D. D. Vuong et al. (Vuong et al., 2004). They observed evolution of tin oxide crystals from 1 to 36 h as coarsening in crystallite size from 6 to 7.5 nm, respectively.

4. CONCLUSIONS

In conclusion, nanosized SnO_2 powder was synthesized by a hydrothermal treatment of precipitated hydrous tin oxide gel suspended in an aqueous ammonium hydroxide solution.

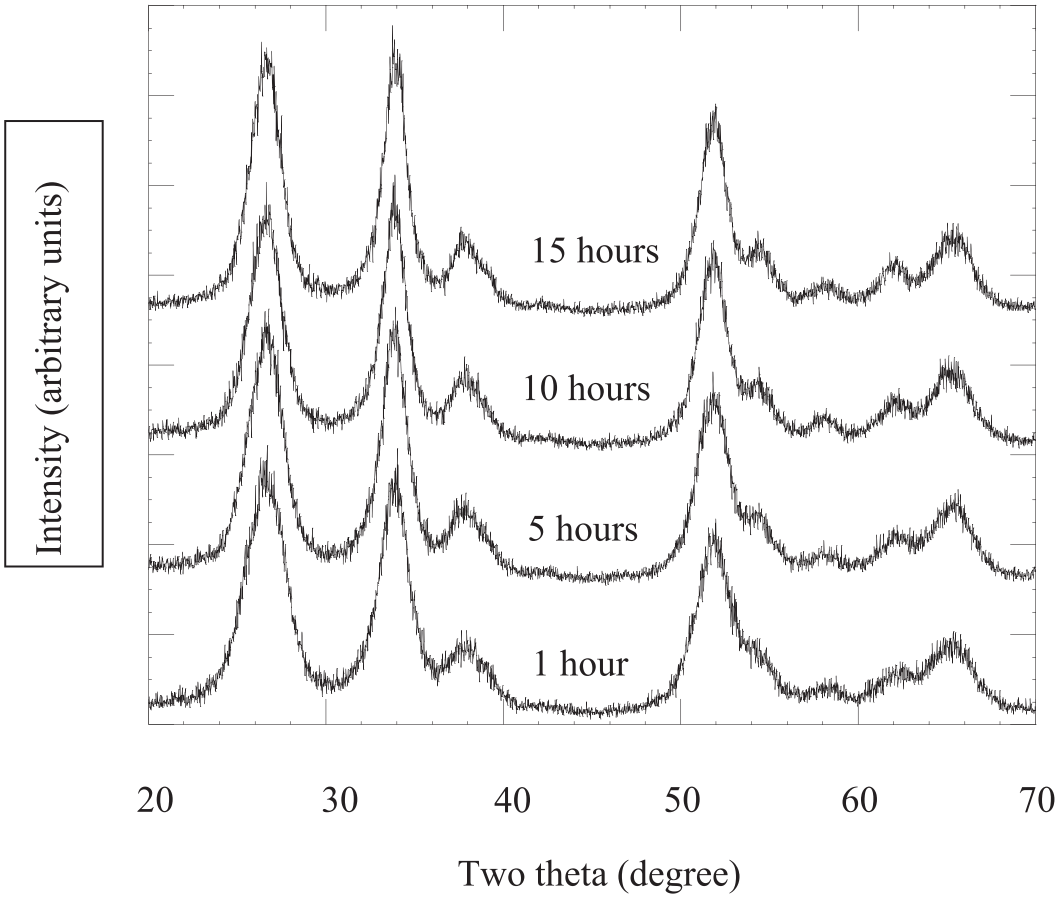

Figure 7. XRD pattern of 1, 10 and 15 h synthesized 0.05 M SnO_2 powder

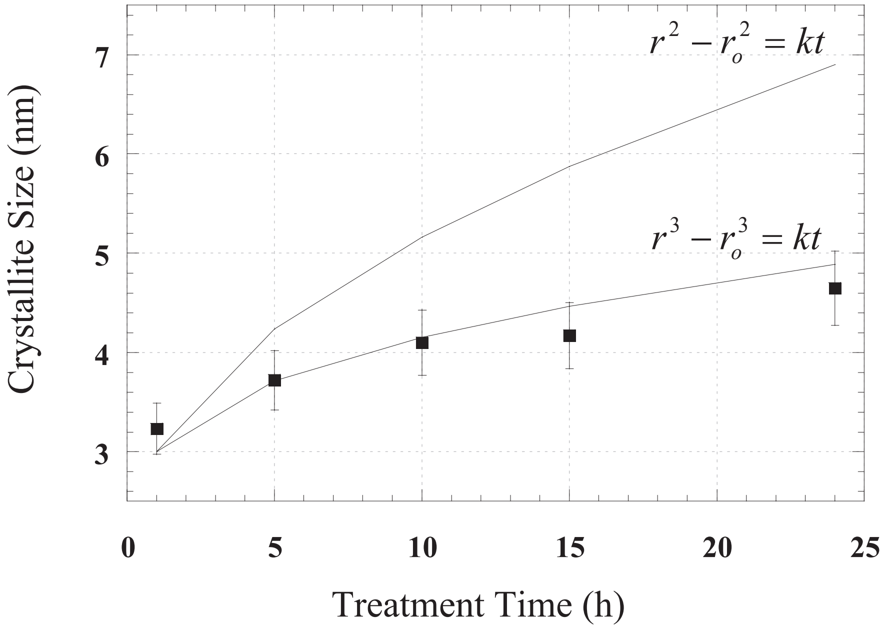

Figure 8. Effect of treatment time on crystallite size of SnO_2 powder

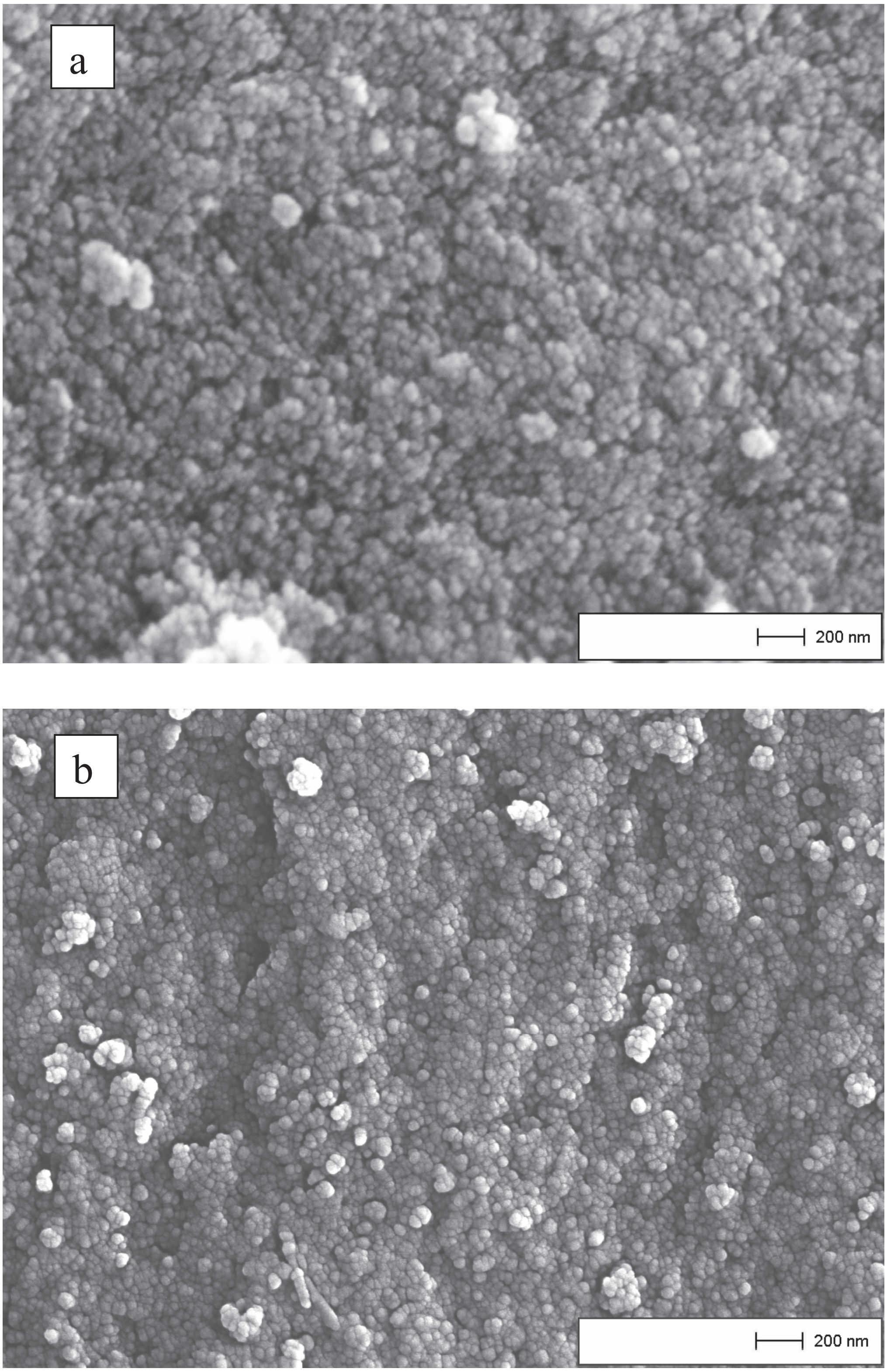

Figure 9. SEM micrograph of the SnO_2 powder synthesized at 200°C for a) 1 h, b) 24 h

It has been also shown that the initial $SnCl_4$ concentration and treatment time have significant effect on the powder characteristics. As the initial hydrous tin oxide concentration increases, the crystallite size increases due to Ostwald ripening type growth process whereas the specific surface area decreases. Similarly, increasing the treatment time results in a significant increase in the crystallite size due to diffusion controlled growth process and a decrease in the specific surface area of the synthesized SnO_2 powder. This understanding on formation mechanism of SnO_2, developed in this study has been successfully utilized to tailor powder characteristics of the SnO_2 particles as predicted from the SEM and the BET results. This understanding may expand the application areas of nanosized SnO_2 powders and enable us to produce high performance gas sensors for future sensing applications.

ACKNOWLEDGEMENTS

The authors would like to thank Mr. Göktuğ Günkaya and Mr. Özgür Özer for fruitful discussions throughout this study. In addition, they would like to thank Ms. Esin Apaydın for her help during the FTIR analysis and Dr. Meryem Sakızcı for her help during the BET analysis. The financial support from Anadolu University Scientific Research Projects Commission (under the contract number: 010263), TUBITAK Career Project (104M279) and Turkish State Planning Organization (DPT 2003-K120170) for this study is also gratefully acknowledged. One of the authors, Ender Suvaci, also thanks to Turkish Academy of Sciences (TUBA) for their financial support through TUBA-Outstanding Young Investigator (GEBIP) Programme.

REFERENCES

Aoki, A. and Sasakura, H. (1970). Tin oxide thin film transistors. *Jpn. J. Appl. Phys*. 9, 582.

Baik, N.S. and Sakai, G. (2000). Hydrothermally treated sol solution of tin oxide for thin-film gas sensor. *Sensors and Actuators B*. 63, 74–79.

Baik, N.S., Sakai, G., Miura, N. and Yamazoe, N. (2000). Preparation of stabilized nanosized tin oxide particles by hydrothermal treatment. *J. Am. Ceram. Soc*. 83, 2983-2987.

Bhagwat, M., Shah, P. and Ramaswamy, V. (2003). Synthesis of nanocrystalline SnO_2 powder by amorphous citrate route. *Materials Letters*. 57, 1604-1611.

Caldadararu, M., Popa, V.T. and Ionescu, N.I. (1995). Surface dynamics in tin dioxide-containing catalysts I. Surface dynamics of tin dioxide interaction with propene-containing feed in presence of residual water, *Appl. Catal*. A. 125, 247.

Chopra, K.L., Major, S. and Pandya, D.K. (1983). Transparent conductors - a status review. *Thin Solid Films*. 102, 1-46.

Cullity, B.D. (1978). *Elements of x-ray diffraction*. Addison-Wesley Pub. Co, Reading, Mass.

Dawar, A.L. and Joshi, J.C. (1984). Semiconducting transparent thin films: their properties and applications. *J. Mater. Sci*. 19 1–23.

Feng, L., Liying, C., Zhiqiang, C., Jiaqiang, X., Jianmin, Z. and Xinquan, X. (2002). Two-step solid-state synthesis of tin oxide and its gas-sensing property. *Materials Chemistry and Physics*. 73, 335-338.

He, Y. and Li, Y. (1999). Chemical control synthesis of nanocrystalline SnO_2 by hydrothermal reaction. *Materials Letters* 40, 23–26.

Henrich, V.E. and Cox, P.A. (1994). *The Surface Science of Metal Oxides*. Cambridge University Press, Cambridge.

Hirano, S. (1987). Hydrothermal processing of ceramics. *Am. Ceram. Soc. Bull*. 66(9), 1342-44.

Ihokura K. and Watson, J. (1994). *The Stannic Oxide Gas Sensor-Principles and Apllications*. CRC Pres, Boca Raton, FL.

Ihokura, K. (1981). New Mater. *Proc*. 1, 43.

Lee, J.H. and Park, S.J. (1993). Preparation of spherical SnO_2 powders by ultrasonic spray pyrolysis. *J. Am. Ceram. Soc*. 76, 777-780.

Lifshitz, I.M. and Slyozov, V.V. (1961). The kinetics of precipitation from supersaturated solid solutions. *J. Phys. Chem. Solids*. 19, 35-50.

Moulson, A.J. and Herbert, J.M. (1990). *Electroceramics*, New York, Chapman & Hall.

Nielsen, A.E. (1964). *Kinetics of precipitation*, Pergamon, Oxford.

Nitta, N. and Otani, S. (1980). Temperature dependence of resistivity of Sn-based gas sensors exposed to CO, H_2 and C_3H_8 gases. *J. Electron. Mater*. 9(4), 727-743.

Pianaro, S.A., Bueno, P.R. and Varela, J.A. (1995). A new SnO_2-based varistor system. *J. Mater. Sci. Lett*. 14, 692–694.

Popescu, D.A. and Verduraz, F.B. (2001). Infrared studies on SnO_2 and Pd/SnO_2. *Catalysis Today*. 70, 139-154.

Ring, T.A. (1996). *Fundamentals of ceramic powder processing and synthesis.* Academic Pres.

Seiyama, T., Egashira, M., Sakamoto, T. and Aso, I. (1972). Oxidative dehydroaromatization : II. Oxidation of propylene over binary oxide catalysts containing bismuth or tin, *J. Catal*. 24, 76.

Seiyama, T., Kato, A., Fujiishi, K. and Nagatani, N.A. (1962). New Detector for Gaseous Components Using Semiconductive Thin Films. *Anal. Chem*. 34, 1502.

Socrates, G. (1980). *Infrared Characteristic Group Frequencies*, Wiley, New York. 145.

Song, K.C. and Kang, Y. (2000). Preparation of high surface area tin oxide powders by a homogeneous precipitation method. *Materials Letters*. 42, 283-289.

Song, K.C. and Kim, J.H. (1999). Preparation of nanosize tin oxide particles from water-in-oil microemulsions. *Journal of Colloid and Interface Science*. 212, 193-196.

Taguchi, N. (1962). Japenese Patent Application No. 45-38200.

Vuong, D.D., Sakai, G., Shimanoe, K. and Yamazoe, N. (2004). Preparation of grain size-controlled tin oxide sols by hydrothermal treatment for thin film sensor application, *Sensors and Actuators B* 103, 386–391.

Xu, C., Tamaki, J., Miura, N. and Yamazoe, N. (1990). Relationship between gas sensitivity and microstructure of porous SnO_2. *Denki Kagaku*. 58, 1143.

Yamazoe, N., Fuchigami, J., Kishikawa, M. and Seiyama, T. (1979). Interactions of tin oxide surface with O_2, H_2O and H_2. *Surf. Sci*. 86, 335.

Zhang, G. and Liu, M. (1999). Preparation of nanostructured tin oxide using a sol-gel process based on tin tetrachloride and ethylene glycol. *Journal of Materials Science*. 34, 3213-21.

Zhang, J.P. (2003). Hydrothermal synthesis and characterization of SnO_2 nanoparticles. *Acta Chimica Sinica*. 61(12), 1965-68.